

# Modelling of permanent magnets with the Boundary Element Method

R. Roeckelein and H. A. M. v. d. Berg

Research Laboratories of SIEMENS A G in Erlangen

When Boundary Element Methods are exploited for the numerical calculation of linear magnetostatic fields, a vector potential formulation is mostly applied to deal with two-dimensional problems whereas scalar potentials seem to be more suitable for three-dimensional situations.

This paper shows how permanent magnets can be modelled in this environment. The source terms arising from permanent magnets consist of a curl or divergence of the magnetization depending upon the formulation. For some important practical applications, e.g. unit magnetization with constant or radial direction, these source terms are nonzero only on the surface of the magnets and are therefore modelled by jump conditions for the flux.

A two-dimensional example finds its origin in magneto-optical memories, where a multilayer system is employed to realize direct overwrite. Characteristic of this problem are finite boundary conditions and thin high permeable layers. As another application a three-dimensional calculation was performed for a pole of a permanent magnet. It is shown that a general purpose potential code (BEASY) can be used for such type of calculations.

**Key Words:** boundary elements, finite elements, magnetostatics, permanent magnets, potential formulations

## 1. INTRODUCTION

Permanent magnets are of growing interest in different fields of applied electromagnetic phenomena. Field calculations for this problem type are based on Maxwell's equations, which can often be simplified by static consideration. The influence of some important kinds of permanent magnet distributions can be expressed by source terms only on the boundary of the permanent magnet. The use of potential formulations then leads to Poisson type of equations.

In some practical cases of interest the permeability of the materials can be assumed to be piecewise constant. In these cases the 'Mixed Boundary Element Method'<sup>1</sup> is a good choice compared with other methods, e.g. the Finite Element Method. The robustness, the accuracy, the convenience of the boundary element techniques are tested by means of two practical situations, which are known to be far from optimally suited for this method.

First, a problem that roots in the magneto-optical memories — namely a direct overwrite scheme — is analysed. Second, the classical pole piece with a soft magnetic pole tip is subjected to closer examination. The latter example will be treated also in three dimensions. The performance of the method will be compared to the finite element technique.

For magnetostatic problems without permanent magnets, the Boundary Element approach with an indirect double layer formulation was used in Ref. 2. Two-dimensional finite element modelling of perma-

nent magnets together with a vector potential formulation is presented in Ref. 3. A more theoretical work about surface current distributions and scalar potentials is given in Ref. 4. In Ref. 5 the advantages and disadvantages for the different boundary element formulations together with a proposal for an economic solution are pointed out.

The formulation chosen herein makes it possible to handle permanent magnets straightforwardly and to use a commercially available, general purpose Boundary-Element program (BEASY<sup>6</sup>), which is not specialized for magnetic field computations.

## 2. BOUNDARY REPRESENTATION OF PERMANENT MAGNETS

In this section we show that some kinds of permanent magnet distributions can be represented by either a current or a charge density at the boundary of the magnet only.

We start from the basic equations of magnetostatics. We separate the permanent magnetization  $\mathbf{M}_p$  from the magnetization resulting from permeability, being eventually inhomogeneous and nonlinear:

$$\operatorname{div} \mathbf{B} = 0 \quad (1)$$

$$\operatorname{rot} \mathbf{H} = \mathbf{J} \quad (2)$$

$$\mathbf{B} = \mu_0 (\mu_r \mathbf{H} + \mathbf{M}_p) \quad (3)$$

where  $\mathbf{B}$ ,  $\mathbf{H}$ ,  $\mathbf{J}$ ,  $\mu_0$ ,  $\mu_r$  and  $\mathbf{M}_p$  are the magnetic flux density, the magnetic field, the electric current density, the

permeability in air, the relative permeability and the permanent magnetization, respectively.

The discontinuity conditions across the surfaces (volumes of different permeability) for the field quantities are

$$\mathbf{n} \times (\mathbf{H}_2 - \mathbf{H}_1) = \mathbf{J}_s, \quad (4)$$

$$\mathbf{n} \cdot (\mathbf{B}_2 - \mathbf{B}_1) = 0 \quad (5)$$

with  $\mathbf{n}$  being the outwardly directed unit vector normal to the surface  $S$  of the volume  $V$ ,  $\mathbf{J}_s$  being the local surface current density,  $\mathbf{H}_2 - \mathbf{H}_1$  and  $\mathbf{B}_2 - \mathbf{B}_1$  being the differences of  $\mathbf{H}$  and  $\mathbf{B}$  on the surface from inside and outside the volume.

To solve the above equations, it is convenient to fulfill implicitly one of the equations (1) or (2) by introducing basic functions or potential formulations. The coupling equation (3) can then be used to eliminate the other equation of (2) or (1).

The substitution of  $\mathbf{B}$  from (3) into (1) leads to

$$\text{div}(\mu_r \mathbf{H}) = -\text{div} \mathbf{M}_p \quad (1')$$

Analogously we get by substituting  $\mathbf{H}$  of (3) into (2)

$$\text{rot}((1/\mu)\mathbf{B}) = \mathbf{J} + \text{rot}((1/\mu_r)\mathbf{M}_p), \text{ with } \mu = \mu_0\mu_r. \quad (2')$$

$\mathbf{M}_p$  is nonzero only in the volume of the permanent magnet. At the boundary of  $V_p$  we get from (4) and (5) a surface charge density  $\rho_m$  or a surface current density  $\mathbf{J}_m$  due to the jump in the permanent magnetization

$$\rho_m = N_p \cdot \mathbf{n} \quad (\text{magnetic surface charge density}) \quad (6)$$

$$\mathbf{J}_m = ((1/\mu_r)\mathbf{M}_p) \times \mathbf{n} \quad (\text{magnetic surface current density}) \quad (7)$$

$\mathbf{n}$  is the outwardly directed unit vector normal to the surface of  $V_p$ . If  $\text{div}(\mathbf{M}_p)$  or  $\text{rot}((1/\mu_r)\mathbf{M}_p)$  are zero in the interior of the magnet volume, the impact of the permanent fraction  $\mathbf{M}_p$  is fully defined by (6) and/or (7).

Let us present a few examples of technical importance that exhibit this feature. First we look for constant permanent magnetization in an arbitrary volume  $V_p$  (Fig.1).

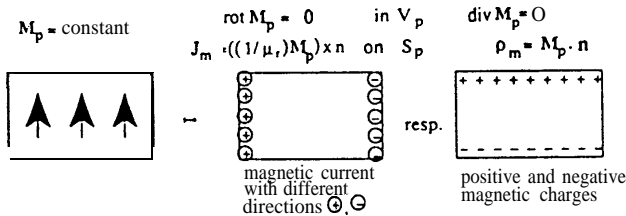


Fig.1. Representation of constant magnetization

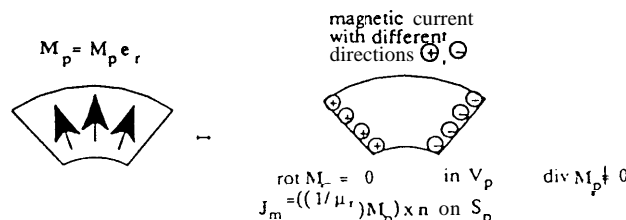


Fig.2. Representation of radial magnetization  $\mathbf{M}_p = M_p \mathbf{e}_r$  ( $\mathbf{e}_r$  - unit radial vector)

For constant  $\mu_r$ , both the  $\text{rot}((1/\mu_r)\mathbf{M}_p)$  and the  $\text{div}(\mathbf{M}_p)$  term are zero inside  $V_p$ , and so both terms can be represented by current or charge densities on the boundary  $S_p$ .

Furthermore radially directed magnetization with constant magnitude often occurs in practice (Fig. 2). Here only  $\text{rot}((1/\mu_r)\mathbf{M}_p)$  vanishes in the interior of  $V_p$ , when  $\mu_r$  is constant, while the  $\text{div}(\mathbf{M}_p)$  term is nonzero.

### 3. POTENTIAL FORMULATIONS FOR MAGNETOSTATICS

In general, two types of potential formulations have proven to be of much benefit to the stationary electromagnetic problem. First, there is the total scalar potential  $\Phi$ , being optimally suited to cover objects that do not carry current. Then the field  $\mathbf{H}$  is given by  $\mathbf{H} = -\text{grad} \Phi$  and equation (1') transforms into

$$\text{div}(\mu_r \text{grad} \Phi) = \text{div} \mathbf{M}_p, \quad (8)$$

while equation (2) is implicitly satisfied.

A modification of  $\Phi$  is the reduced scalar potential  $\Phi_m$ . Each vector field, and thus  $\mathbf{H}$ , can be decomposed into a solenoidal part  $\mathbf{H}_c$  and an irrotational component  $\mathbf{H}_m$ , associated with the magnetization, which satisfies  $\mathbf{H}_m = -\text{grad} \Phi_m$ .

According to equation (1') we obtain:

$$\text{div}(\mu_r \text{grad} \Phi_m) = \text{div}(\mathbf{M}_p) + \text{div}(\mu_r \mathbf{H}_c). \quad (9)$$

When  $\mu_r$  is piecewise constant, the  $\text{div}(\mu_r \mathbf{H}_c)$  term reduces to zero inside each part (see equation (1)) and only a surface contribution remains on the boundaries between regions with different permeability.

#### Vector potential

A vector potential formulation is well suited for two-dimensional problems or when eddy currents have to be taken into account. Introduction of a vector potential  $\mathbf{A}$  with  $\mathbf{B} = \text{rot} \mathbf{A}$  satisfies equation (1), whereas (2') transforms into

$$\text{rot}((1/\mu)\text{rot} \mathbf{A}) = \mathbf{J} + \text{rot}((1/\mu_r)\mathbf{M}_p). \quad (10)$$

By assuming two-dimensional field distributions equation (8) simplifies to

$$\text{div}((1/\mu)\text{grad} A) = -J - \text{rot}((1/\mu_r)\mathbf{M}_p) \quad (11)$$

for the component of  $\mathbf{A}$  and  $\mathbf{J}$  perpendicular to the 2D plane. Again, we arrive at the Poisson equation.

### 4. THE BOUNDARY ELEMENT METHOD (BEM)

The application of the BEM for numerically solving the various types of partial differential equations has made good progress in the last years. Mostly elliptic partial differential equations, e.g. coming from static structural mechanics, are solved with this method. Potential formulations for magnetostatics often lead to Poisson equations (see section 3.):

$$\text{div} \epsilon \text{grad} \Psi = b \quad (12)$$

where  $\Psi$ ,  $b$  and  $\epsilon$  are a potential, a source density and a material constant, respectively.

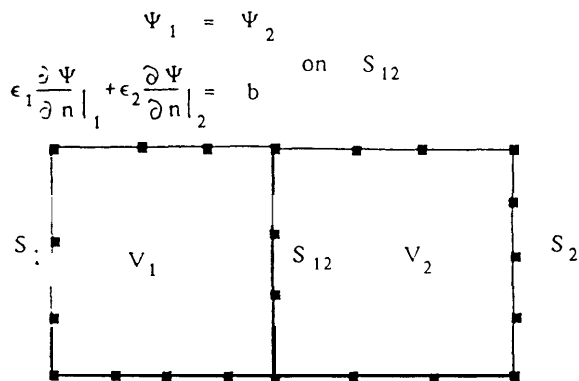


Fig. 3. Modelling of sources on the boundaries by coupling the flux densities

The mixed boundary integral equation for this problem with  $\epsilon$  constant is

$$c \cdot \Psi + \int_S \Psi \frac{\partial G}{\partial n} ds - \int_S \frac{\partial \Psi}{\partial n} G ds = - \frac{1}{\epsilon} \int_V b \cdot G dV \quad (13)$$

$V$  is the domain of computation with boundary  $S$ ,  $n$  the outwardly directed unit-vector normal to  $S$  and  $G$  is the Green's Function for (12).  $c$  depends on the dimension of the problem and the geometry of the boundary.

For different piecewise constant material quantities we can set up (13) for each zone. On the zone boundaries the potential is continuous. With no sources on the boundary the normal flux density is continuous as well. For sources on the boundary the sum of the normal flux density from both sides must be equal to the source density.

Consequently, source terms inside a zone can be modelled by the volume integral on the right hand side of (13), whereas source terms on zone boundaries are represented by coupling the flux densities (Fig. 3).

For point or line sources in the interior of a zone the volume integral in equation (13) can be evaluated quite easily.

The boundary is approximated by subdivision into simple elements (e.g. lines, triangles or quadrilaterals).  $\Psi$  and  $\partial\Psi/\partial n$  are represented by a combination of basis functions (e.g. piecewise polynomials) and equation (13) is approximated by point matching for the boundary points.

On the boundary of the domain  $V$  we get one, on zone interfaces  $S_{ij}$  two unknowns per node.

The main advantage of the method is that only the material boundaries must be modelled and that infinite regions can be handled straightforwardly, too. The main disadvantage is that we have to solve domain integrals for some kinds of nonlinearities in the interior of the domain.

### 5. APPLICATIONS

In this section we will discuss the performance of the BEM in two situations of practical significance, which do not excel in that they are well conditioned in the

numerical sense. In these examples, materials with strongly deviating magnetic properties are involved, whereas the geometries are characterized by discontinuous corners and large aspect ratios.

The first calculation concerns a so-called direct-overwrite system for magneto-optic (m. o.) memories. The present m.o. memories suffer from the drawback that, prior to writing, the segments in question on the disk have to be erased so that each such segment has to be traced two times for a single writing operation. The information is written by locally heating up the m.o. information carrier 1 with a focussed laser beam so that the intrinsic anisotropy reduces in that region and the magnetization lines up along the total magnetic field.

After cooling this  $M$  distribution is fixed. Unfortunately it is impossible to alter the magnetic field direction of a coil with sufficient rate in order to be able to impose two different  $M$ -directions, i.e. the two different kinds of bits. A cross section of the present direct overwrite medium is depicted in Fig. 4, and it consists of a layered structure of an m.o. storage medium 1, a soft-magnetic control film 2, a permanent magnetic field source 3 in form of a magnetic film with magnetization perpendicular to the film surface, and, finally, a transparent nonmagnetic substrate. The groove structure in the substrate, which serves as tracking guide of the optical head, is exploited to realize a relief in the field-source layer so that it induces a fringing field outside. In principle, the control layer screens these fringing fields of layer 3 so that only the field source I is effective in producing a field at the heated spot in the storage layer. When a higher laser power is used, the temperature of the control layer increases locally above its Curie temperature and the field of layer 3 can penetrate via this hole in the soft-magnetic shield into the heated region of the storage layer. The total Maxwell field inverts and the opposite  $M$ -direction is fixed after cooling.

A two-dimensional model, in which the parameters are constant along the track, is employed to simulate both above situations. A cross-section of the track is given in Fig. 5a. For simplicity it has been assumed that the paramagnetic holes in the control layer constitute a

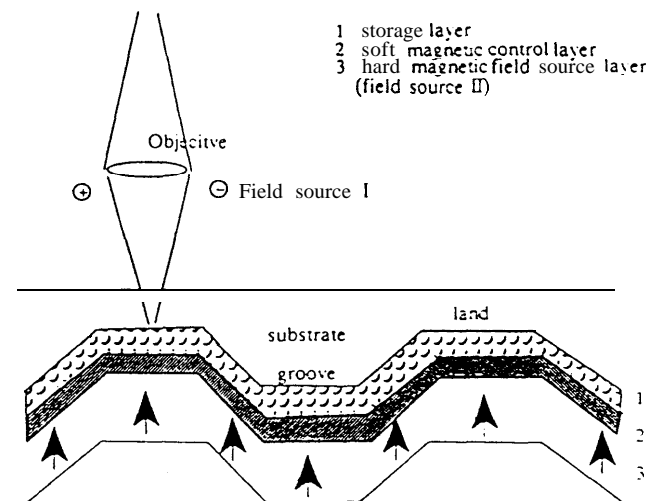


Fig. 4. A cross section of the storage disk perpendicular to the data tracks

periodic pattern centred symmetrically either with respect to the groove or to the land regions (see Fig. 4). Consequently, the lateral field components are zero at the left and right boundary in Fig. 5a. The relative permeability has been taken equal to one for all media, except for the soft-magnetic control layer with  $\mu_r=1000$ . In the paramagnetic regions of 2,  $\mu_r$  has been put equal to one. Figs 5a and 5b illustrate the big difference in complexity between the networks of the boundary and the finite element technique, respectively.

The following questions are of main importance: Firstly, what field magnitude can be achieved in the

critical region of the storage layer for a given saturation magnetization of layer 3? Secondly, what is the optimal geometry of the groove structure and, finally, what is the minimal thickness of the soft-magnetic control layer 2 so that no saturation of this layer occurs?

Figure 6a shows the stray-field pattern in the middle of the storage layer. Of course, its magnitude and spatial distribution depend on the expanse of paramagnetic holes. Typically, the minimal value of the vertical field component is larger than  $0.05M_p$ , which yields about 40 kA/m for practical materials. For this, the groove depth should be about three times larger than in a standard disk.

Figure 6b demonstrates the good similarity in the results obtained by exploiting the referred numerical methods and formulations (FEM with vector potential, BEM with vector and scalar potential) for the sensitive locations just outside the soft-magnetic layer without gap.

Figure 7 indicates a maximum in the magnetization in layer 2 at the groove edge when no paramagnetic holes are present. For realistic materials, the control-layer thickness should be in the order of 100 nm to prevent saturation from occurring.

The Boundary Element Method (BEM) needs discretization of zone and exterior boundaries only, whereas for the Finite Element Method (FEM) the permeable and air parts have to be discretized with

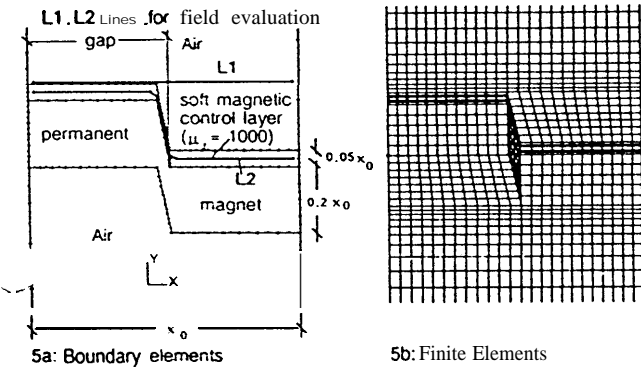


Fig. 5. Discretized model

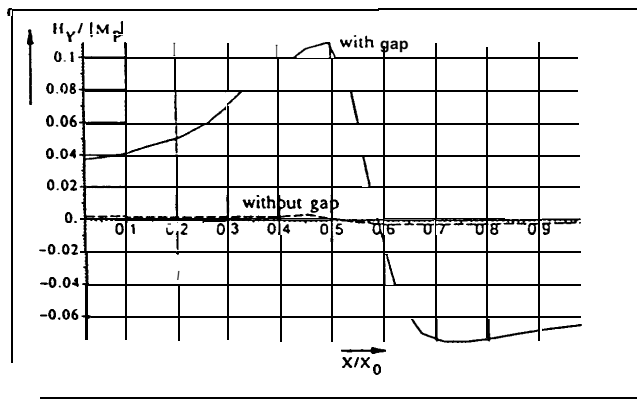


Fig. 6a. Vertical magnetic field component with and without gap

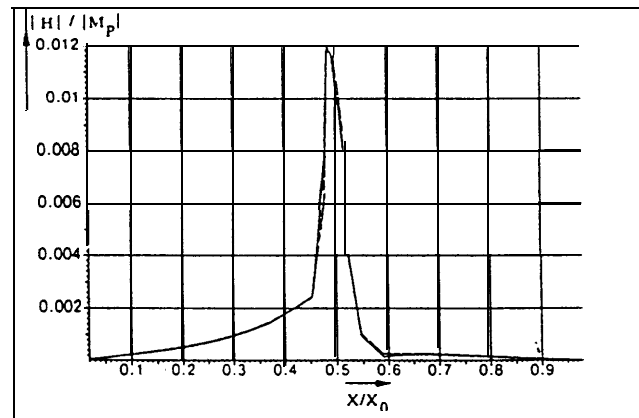


Fig. 7. Magnetic field inside the high-permeable control layer (Line L2 in Fig. 5a). Results for FEM with vector potential and BEM with vector and scalar potential are practically identical

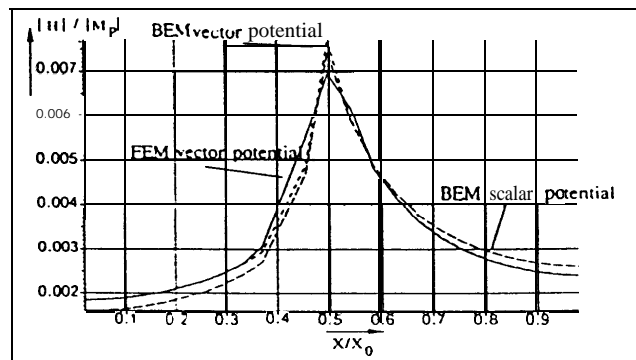


Fig. 6b. Comparison of the magnetic field without gap for different formulations and methods

Fig. 6. Results at the height of the land region of the storage layer (Line L1 in Fig. 5a)

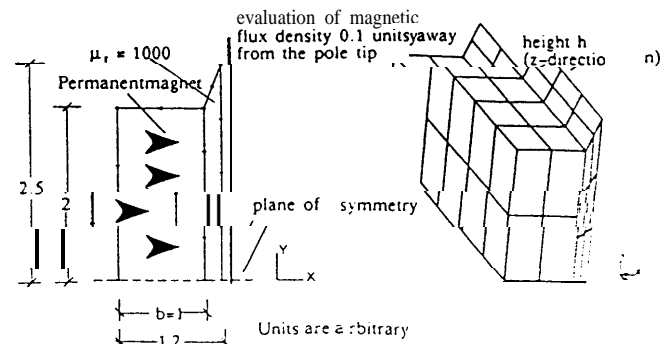


Fig. 8. 3D model and discretization for a permanent magnet with a pole tip

triangles or quadrilaterals. This reduces the topological dimension of the model geometry by one and is responsible for an easy integration into a CAD (Computer Aided Design) process and a faster model creation phase.

The processing time for setting up and solving the system matrix shows almost no difference in this example. With boundary elements, we have fewer unknowns, but nonsymmetric and dense matrices, whereas with finite elements the system matrix is sparse and symmetric.

For results evaluation with both methods we get potential and flux values for the discretization nodes. Thus with FEM we automatically get a good representation of the results in the whole domain, which is useful e.g. for extremum evaluation or for the drawing of flux lines. With BEM we can calculate the results afterwards at any desired location (see equation (11)). A flux line evaluation, however, is not possible in an as similar and straightforward way as with finite elements.

Some integral equation formulations have problems with accuracy near the boundaries of high permeable or rather thin layers<sup>4</sup>. With the mixed BEM together with analytic or equivalent accurate element integration we get good results inside and outside near to the surface of the layer (see Fig. 6). With BEM the two scalar and the vector potential formulation were used. These are known to be an upper and lower bound for the exact solution in some sense<sup>7</sup>. Near the discontinuity of the geometry the BEM results are more reliable, because finite elements are known to average discontinuities depending on the degree of discretization.

A simple 3D example with total scalar potentials is shown in Fig. 8. It simulates a permanent magnet block with a pole tip of high permeable material. Again we can see that we get good results near the pole tip surface (Fig. 9).

All the boundary element calculations above were performed with a general purpose, commercially available boundary element program (BEASY<sup>6</sup>). BEASY has a rather flexible element library for two- and three-dimensional problems. It can be used to solve the Poisson equation with the mixed Boundary Element approach as described in section 4. We get two unknowns for each interface node and the resulting equation system is solved simultaneously. This is of course not so

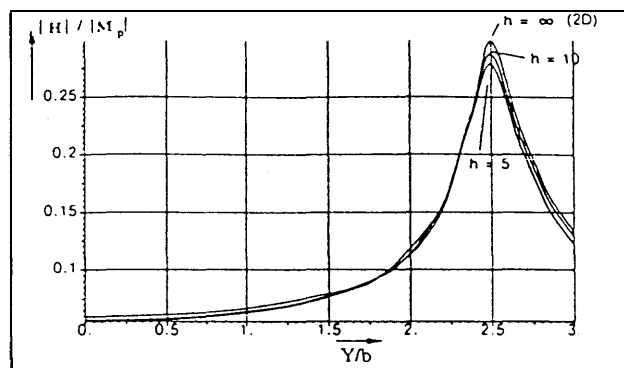


Fig. 9. Magnetic field 0.1 units away from the pole tip for different values of height  $h$  (see Fig. 8)

economic as solving two systems of half the size as proposed in Ref. 5. But BEASY is well suited also for other problem types (e.g. structural mechanics, thermal problems) and is well integrated into CAD. Therefore it is not feasible to put effort in developing special magnetic programs for solving this type of problems.

## REFERENCES

- 1 Brebbia, C. A., Telles, J. and Wrobel, L. *Boundary Element Techniques*, Springer-Verlag, Berlin-Heidelberg-New York-Tokyo, 1984
- 2 Armstrong, A. G. M., Simkin, J. and Trowbridge, C. W. The Galerkin method of weighted residuals applied to the restricted magnetostatic scalar-potential boundary-integral equation in three dimensions, *IEEE Trans. on Magn.*, 1983, **19** (6)
- 3 Brauer, J. R., Larkin, L. A. and Overbye, V. D. Finite element modeling of permanent magnet devices, *J. Appl. Phys.*, 1984, **55** (6)
- 4 Ciric, I. R. New models for current distributions and scalar potential formulations of magnetic field problems, *J. Appl. Phys.*, 1987, **61** (8)
- 5 Lindholm, D. Notes on boundary integral equations for three-dimensional magnetostatics, *IEEE Trans. on Magn.*, 1980, **MAG-16** (6)
- 6 BEASY—Boundary element analysis system, user's manual version 3.00, Fa. CM—BEASY, Southampton
- 7 Penman, J. and Fraser, J. R. Complementary and Dual Energy Finite Element Principles in Magnetostatics, *IEEE Trans. on Magn.*, 1982 **MAG-18**, (2)